Journal of Materials Chemistry A

PAPER

View Article Online
View Journal

Cite this: DOI: 10.1039/c5ta06042g

Plasticizing Li single-ion conductors with low-volatility siloxane copolymers and oligomers containing ethylene oxide and cyclic carbonates†

Siwei Liang,[ab] Quan Chen,‡[ac] U Hyeok Choi,[ad] Joshua Bartels,[a] Nanqi Bao,[a] James Runt[a] and Ralph H. Colby*[a]

Received 3rd August 2015
Accepted 9th September 2015

DOI: 10.1039/c5ta06042g

www.rsc.org/MaterialsA

To prepare a safe electrolyte for lithium ion batteries, two groups of novel low-volatility plasticizers combining pendant cyclic carbonates and short ethylene oxide chains have been successfully synthesized, as confirmed by ^{1}H, ^{13}C and ^{29}Si NMR spectroscopy. The Fox equation describes the composition dependence of the glass transition temperature (T_g) very well for the random polysiloxane-based copolymer plasticizers (11 000 < M < 13 000) while the smaller oligomer plasticizers have T_g as much as 20 K lower than the Fox equation prediction because of their lower molecular weight (450 < M < 700). The Landau–Lifshitz mixing rule describes the dielectric constant of the random polysiloxane-based copolymer plasticizers at all temperatures above T_g. Mixing with 20 wt% polysiloxane tetraphenyl borate – Li ionomer (14 mol% borate and 86 mol% cyclic carbonate) increases conductivity relative to the neat ionomer by lowering T_g, increasing dielectric constant and providing better solvation of Li$^+$. The best oligomeric plasticizer only has T_g 10 K lower than the Fox prediction but has dielectric constant 30% larger than expected by the Landau–Lifshitz mixing rule, owing to a surprisingly low viscosity, resulting in ambient conductivity 2 × 10^{-5} S cm^{-1}. For both groups of plasticizers, the fraction of cyclic carbonates relative to ethylene oxide governs the magnitude and temperature dependence of the ionic conductivity.

Introduction

Polymer electrolytes as energy materials are of great interest for lithium-ion battery, fuel cell, solar cell and ionic actuator applications, due to the inherent polymeric merits, such as mechanical robustness and ease of processing to make thin-film membranes. Among different types of polymer electrolytes, single-ion conductors with one type of ion covalently bonded to the polymer have recently attracted increased attention, owing to (1) high selectivity of conducting ions (lithium ion transference number near unity) and (2) elimination of anion polarization at the electrode/electrolyte interface that weakens the electric field inside the electrolyte and causes safety problems.[1–6]

Ionomers with weak binding borate anions are particularly useful as cation conductors.[7–10] Since the boron is less electronegative than carbon, B is positive and the negative charge is delocalized, weakening the ion pair energy with Li$^+$ and other cations.[11,12] Recently developed novel tetraphenyl borate – Li polysiloxane single-ion conductors[13] with cyclic carbonate side chains were shown to have exceptionally low conducting ion activation energy (7–10 kJ mol^{-1}) from the weak binding between delocalized anions and Li$^+$ and the strong solvation of Li$^+$ from the carbonate oxygens. The nonionic polysiloxane homopolymer with only cyclic carbonate side chains has dielectric constant ~50 near room temperature, further weakening the ionic interactions. However, it seems that the large tetraphenyl borate anions repel the cyclic carbonate side chains, effectively aggregating the ions on the nanoscale, which raises T_g, lowers segmental mobility, and traps the majority of the Li$^+$ ions in aggregates, with only between 1% and 5% of the Li$^+$ ever participating in conduction, as seen in the infinite temperature intercept of the Arrhenius simultaneously conducting Li$^+$ content.[13]

Addition of polar solvating plasticizers can improve the conductivity through three effects: (1) lowering T_g to improve ionic mobility, (2) raising dielectric constant to weaken the ionic interactions and (3) providing specific solvation of Li$^+$, with the former one to enhance ionic mobility and the latter two to increase participation of Li$^+$ in conduction. By simply

[a]Materials Science and Engineering, The Pennsylvania State University, University Park, PA 16802, USA. E-mail: rhc@plmsc.psu.edu

[b]Joint Center for Artificial Photosynthesis, Lawrence Berkeley National Laboratory, One Cyclotron Road, Berkeley, CA 94720, USA

[c]State Key Laboratory of Polymer Physics and Chemistry, Changchun Institute of Applied Chemistry, Chinese Academy of Sciences, Changchun 130022, China

[d]Functional Composites Department, Korea Institute of Materials Science, Changwon, 642-831, Korea

† Electronic supplementary information (ESI) available: Composition of copolymer plasticizers and NMR spectra of all plasticizers. See DOI: 10.1039/c5ta06042g

‡ Co-first author.

crosslinking the polyelectrolytes swollen in polar solvating plasticizers, one makes so-called gel electrolytes.[14–19] When mixing with single-ion conductors, plasticizers appear to solvate and transport Li^+ cations more efficiently. In particular, cyclic carbonates such as propylene carbonate (PC) and ethylene carbonate (EC) have been widely used in the Li-ion battery industry, due to their high dielectric constant, strong solvation of Li^+ and ability to form a stable electrode–electrolyte interfacial layer. However, safety issues caused by leakage and evaporation of these small-molecule carbonates prompt scientists to pursue non-volatile alternatives. Poly(ethylene glycol) (PEG) is considered as a good candidate because it can break ion aggregates and solvate cations: when Li^+ leaves an ion aggregate, the ether oxygen of PEG can solvate and stabilize the free Li^+.[20–28] Recently, PEG with molecular weight of 600 g mol^{-1} has been shown to greatly enhance conductivity of polysiloxane tetraphenyl borate-Li single-ion conductors with cyclic carbonate side chains;[22] although crystallization of the PEG oligomers near room temperature led to an abrupt drop in conductivity at lower temperatures when more than ~40 wt% PEG was added.

This paper explores novel plasticizers of low-volatility at working conditions of lithium-ion batteries. They are composed of ether-oxygen units (low T_g, moderate polarity and strong specific solvation of Li^+) and cyclic carbonate units (higher T_g, higher polarity and similar strong solvation of Li^+) with molecular weight $450 < M < 12\,000$. The composition of the low-volatility plasticizers was carefully tuned. Blends of these plasticizers with 20 wt% of a tetraphenyl borate – Li polysiloxane single-ion conductor exhibit improved ionic conductivity up to 2×10^{-5} S cm^{-1} at 25 °C. Furthermore, all the plasticizers and their mixtures with the ionomer are strictly amorphous, allowing a wider temperature range for applications.

Experimental

Materials

Dichloromethane, diethyl carbonate, chlorodimethylsilane, triethyl amine (NEt_3), tetraethylene glycol, potassium carbonate, 2-(2-(vinyloxy)ethoxy)ethanol, diethyl carbonate, toluene and anhydrous acetonitrile were purchased from VWR and used without further purification. Platinum divinyltetramethyldisiloxane complex (Pt[dvs]) (3% in xylene) catalyst, diethyldihydrosilane, tri(ethylene glycol) divinyl ether, di(ethylene glycol) divinyl ether, $RhCl(PPh_3)_3$ catalyst and polymethylhydrosiloxane (PMHS, $M_n = 3360$) were purchased from Aldrich and used as received. Tetrahydrofuran (THF) from EMD Chemicals was refluxed over sodium metal before use. The polysiloxane-based ionomer was prepared by the method reported in ref. 13 with borate content of 14 mol%.

Characterization

^1H, ^{13}C and ^{29}Si NMR spectroscopy were recorded on a Bruker AM 300M spectrometer. Glass transition temperatures (T_g) were determined using a TA Q100 differential scanning calorimeter (DSC) at 10 K min^{-1} heating and cooling rates. Dielectric relaxation spectroscopy (DRS) measurements were conducted on samples sandwiched between two polished brass electrodes, with 50 μm silica spacers placed in between the two electrodes. The sandwiched samples were positioned in a Novocontrol GmbH Concept 40 broadband dielectric spectrometer and the dielectric permittivity and conductivity were measured using an AC voltage amplitude of 0.1 V and 10^{-2} to 10^7 Hz frequency range. Prior to the DRS measurements, the samples were annealed in the Novocontrol at 120 °C in a heated stream of dry nitrogen for 1 hour to drive off any moisture picked up during loading of these hygroscopic materials. Data were collected in isothermal frequency sweeps from 120 °C to near T_g. Linear viscoelastic measurements were conducted with an Advanced Rheometric Expansion System (ARES-LS, Rheometric Scientific). Parallel plates with diameters of 25 mm were utilized to conduct dynamic frequency sweeps at room temperature (20 °C). Strain amplitudes lower than 0.1 were applied and confirmed to be in the linear response region.

Cyclic [(allyloxy) methyl] ethylene ester carbonic acid (CECA)

CECA was prepared according to the method reported in ref. 13. Potassium carbonate (3 g, 21.7 mmol) was added to a mixture of 3-(allyloxy)-propane-1,2-diol (92.4 g, 0.188 mol) and diethyl carbonate (24.8 g, 0.188 mol). After stirring at 120 °C for 24 h, the mixture was filtered to isolate the solid. The residue was purified by Kügelrohr distillation to yield the pure product as a colorless liquid (23.7 g, 80%). ^1H NMR (in $CDCl_3$), δ(ppm) 5.87 (m, 1H, C=CH), 5.25 (d, 1H, *cis* H of CH_2=C), 5.14 (d, 1H, *trans* H of CH_2=C), 4.86 (m, 1H, CCH(C)O), 4.38–4.55 (m, 2H, CH_2C), 4.06 (m, 2H, OCH_2C=C), 3.60–3.74 (m, 2H, $OCCH_2O$).

Tri(ethylene glycol) allyl methyl ether (vinyl PEO_3)

To a mixture of NaH (1.44 g, 60% in mineral oil) dispersed in 20 mL dry THF was added a solution of tri(ethylene glycol) methyl ether (4.7 mL, 0.03 mol) in 150 mL of THF dropwise at ice-bath temperature. The mixture was stirred for 3 hours before being transferred into a solution of allyl bromide (3.58 g, 0.03 mol) in 20 mL dry THF. The mixture was allowed to react overnight to complete the reaction. The reaction was quenched by ice water and extracted by ethyl acetate (20 mL × 3). The organic phases were combined and condensed by rotavap. The yellowish liquid was then purified by vacuum distillation to yield vinyl PEO_3 (5.5 g, 90%). ^1H NMR (in d6-acetone), δ(ppm) 5.85 (m, 1H, CH=), 5.2, (d, *cis* H of $=CH_2$), 5.1 (d, *trans* H of $=CH_2$), 3.95 (d, 2H, C=CCH_2), 3.8–3.6 (m, 8H, OCH_2CH_2O), 3.35 (s, CH_3).

General procedure for synthesis of homopolymer and random copolymer plasticizers CPP (0, 19 31, 57, 80, 100)

All starting materials were dried using molecular sieves before use. PMHS was added into a pre-dried flask equipped with a condenser. The desired amount of CECA and vinyl PEO_3 were charged into the flask followed by 20 mL anhydrous CH_3CN and 0.2 mL Pt catalyst. The reaction mixture was stirred at 70 °C. The completion of the reaction was confirmed by ^1H NMR. The reaction time was in the range of 2–7 days. The mixture was

condensed by rotovap and the residue was dissolved in toluene and precipitated in hexane 3 times. Afterwards, the product was dried in a vacuum oven at 80 °C for 24 hours.

4,4′-(6,6,21,21-Tetramethyl-2,7,10,13,16,19,25-heptaoxa-6,21-disilahexacosane-1,26-diyl)bis(1,3-dioxolan-2-one) (OP62)

CECA (10.86 g, 0.068 mol), anhydrous CH_3CN (20 mL) and chlorodimethylsilane (7.67 g, 0.081 mol) were added into a pre-dried flask. The mixture was cooled by ice-bath before 0.3 mL Pt catalyst was charged. The mixture was allowed to react overnight to complete the reaction. The solvent was evaporated and the residue was vacuum distilled to obtain 4-((3-(chlorodimethylsilyl)propoxy)methyl)-1,3-dioxolan-2-one as a colorless liquid (15.2 g, 89%). ^{1}H NMR (in d6-acetone), δ(ppm) 4.95 (m, 1H, CCH(C)O), 4.4–4.6 (m, 2H, CH_2C), 3.75 (m, 2H, $CCH_2OCH_2CH_2H_2$), 3.55 (m, 2H, $OCH_2CH_2CH_2$), 1.7 (m, 2H, $OCH_2CH_2CH_2$), 0.9 (m, 2H, $OCH_2CH_2CH_2$), 0.35 (m. CH_3); ^{29}Si NMR (in d6-acetone) 33 (s); (Fig. S2†) ^{13}C NMR (in d6-acetone), δ(ppm) 160, 75.1, 74.8, 74, 73.2, 23, 15, 0.2 (Fig. S3†).

4-((3-(Chlorodimethylsilyl)propoxy)methyl)-1,3-dioxolan-2-one (8.7 g, 0.034 mol) was added dropwise into the mixture of NEt_3 (7.5 g), tetraethylene glycol (6.67 g, 0.034 mol) and 20 mL dry THF over 30 minutes. The reaction mixture was allowed to stir overnight to complete the reaction. The mixture was filtered to remove the solid. The liquid was condensed by rotavap and further dried by vacuum oven to yield OP62 as a brown liquid (13 g). ^{1}H NMR (in d6-acetone), 4.95 (m, 1H, CCH(C)O), 4.4–4.6 (m, 2H, CH_2C), 3.75 (m, 2H, $CCH_2OCH_2CH_2H_2$), 3.63 (s, 16H, OCH_2CH_2O) 3.55 (m, 2H, $OCH_2CH_2CH_2$), 1.7 (m, 2H, $OCH_2CH_2CH_2$), 0.9 (m, 2H, $OCH_2CH_2CH_2$), 0.35 (m. CH_3); ^{29}Si NMR (in d6-acetone) 17.57 (s) (Fig. S4†).

4,4′-(6,6,22,22-Tetraethyl-2,9,12,15,19,26-hexaoxa-6,22-disilaheptacosane-1,27-diyl)bis(1,3-dioxolan-2-one) (OP73)

Diethyldihydrosilane (7.2 g, 0.082 mol), CECA (8.4 g, 0.053 mol) and 10 mL benzene were added into a flask followed by 0.1 g $RhCl(PPh_3)_3$ catalyst. The mixture was stirred at room temperature overnight to complete the reaction. The solvent was evaporated and the residue was vacuum distilled to afford 4-((3-(diethylsilyl)propoxy)methyl)-1,3-dioxolan-2-one as a colorless liquid (20 g, 100%). ^{1}H NMR (in d6-acetone), 4.95 (m, 1H, CCH(C)O), 4.4–4.6 (m, 2H, CH_2C), 3.45 to 3.8 (m, 5H, $CCH_2OCH_2CH_2CH_2$, $OCH_2CH_2CH_2$ and SiH), 1.64 (m, 4H, OCH_2CH2CH_2Si), 1 (m, 6H, $OCH_2CH_2CH_2$ and $SiCH_2$), 0.67 (m, 6H, CH_3); ^{29}Si NMR (in d6-acetone) −1.38 (s) (Fig. S5†).

4-((3-(Diethylsilyl)propoxy)methyl)-1,3-dioxolan-2-one (5 g, 0.02 mol) and tri(ethylene glycol) divinyl ether (2 g, 0.01 mol) were mixed followed by 0.1 g $RhCl(PPh_3)_3$ catalyst. The mixture was stirred at room temperature overnight to complete the reaction. The mixture was washed with cyclohexane to afford the product as a brown liquid (7 g). ^{1}H NMR (in d6-acetone), 4.95 (m, 1H, CCH(C)O), 4.4–4.6 (m, 2H, CH_2C), 3.45 to 3.8 (m, 12H, $CCH_2OCH_2CH_2CH_2$, $OCH_2CH_2CH_2$ and OCH_2CH_2O), 1.64 (m, 4H, $OCH_2CH_2CH_2Si$), 1 (m, 6H, $OCH_2CH_2CH_2$ and $SiCH_2$), 0.67 (m, 6H, CH_3); ^{29}Si NMR (in d6-acetone) 5.25 (s) (Fig. S6†).

4,4′-(6,6,20,20-Tetraethyl-2,9,13,17,24-pentaoxa-6,20-disilapentacosane-1,25-diyl)bis(1,3-dioxolan-2-one) (OP67)

The same procedure as synthesis of OP73 was used with di(ethylene glycol) divinyl ether as the linker. ^{1}H NMR (in d6-acetone), 4.95 (m, 1H, CCH(C)O), 4.4–4.6 (m, 2H, CH_2C), 3.45 to 3.8 (m, 10H, $CCH_2OCH_2CH_2CH_2$, $OCH_2CH_2CH_2$ and OCH_2CH_2O), 1.64 (m, 4H, $OCH_2CH_2CH_2Si$), 1 (m, 6H, $OCH_2CH_2CH_2$ and $SiCH_2$), 0.67 (m, 6H, CH_3) (Fig. S7†).

Results and discussion

Synthesis

Two types of plasticizers were synthesized. The first type is referred to as copolymerized plasticizer (CPP), having $(EO)_3$ side chains and cyclic carbonate side chains, synthesized by hydrosilylation using a method described in our previous work (Scheme 1).[13] The CPP samples are coded according to the fraction f of carbonate-containing units, as determined by the integrated areas of ^{1}H NMR peaks (see Fig. S1 and Table S1† for details). For example, CPP-19 means the copolymerized plasticizer having molar fraction $f = 19\%$ of carbonate containing units.

To further improve the performance of the low-volatility plasticizers, the second type of oligomeric plasticizers (OP) of $450 < M < 700$ were synthesized by condensation reactions (Scheme 2). To better compare with the CPP, an equivalent f' is calculated based on the carbonate : EO ratio. Since the CPPs have carbonate side chains (with one cyclic carbonate group and one EO) and EO side chains (with four EOs), the ratio of carbonate : EO $= f/[f + 4(1 - f)]$. For OP, by defining carbonate : EO $= f'/[f' + 4(1 - f')]$ enables an estimation of f' analogous to f of CPP. OPs are coded according to f', for example OP73 means $f' = 73\%$.

OP62 was synthesized by condensation reaction with triethyl amine as an acid scavenger (Scheme 2(a)). The resulting product with Si–O–C linkages is moisture sensitive. The first attempt to synthesize OP67 and OP73 (Scheme 2(b)) failed because the platinum catalyst that works for most hydrosilylation reactions gave nearly no desired product. The well-known Wilkinson Rh

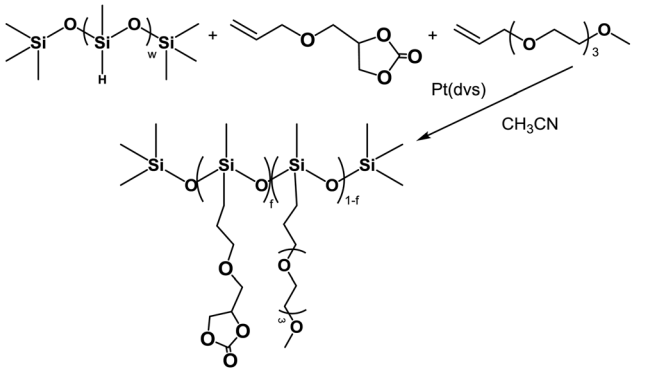

Scheme 1 Synthesis of siloxane random copolymer plasticizers CPP-(0, 19, 31, 57, 80, 100), where the number is the mol% of cyclic carbonate containing units, *i.e.*, 100*f*.

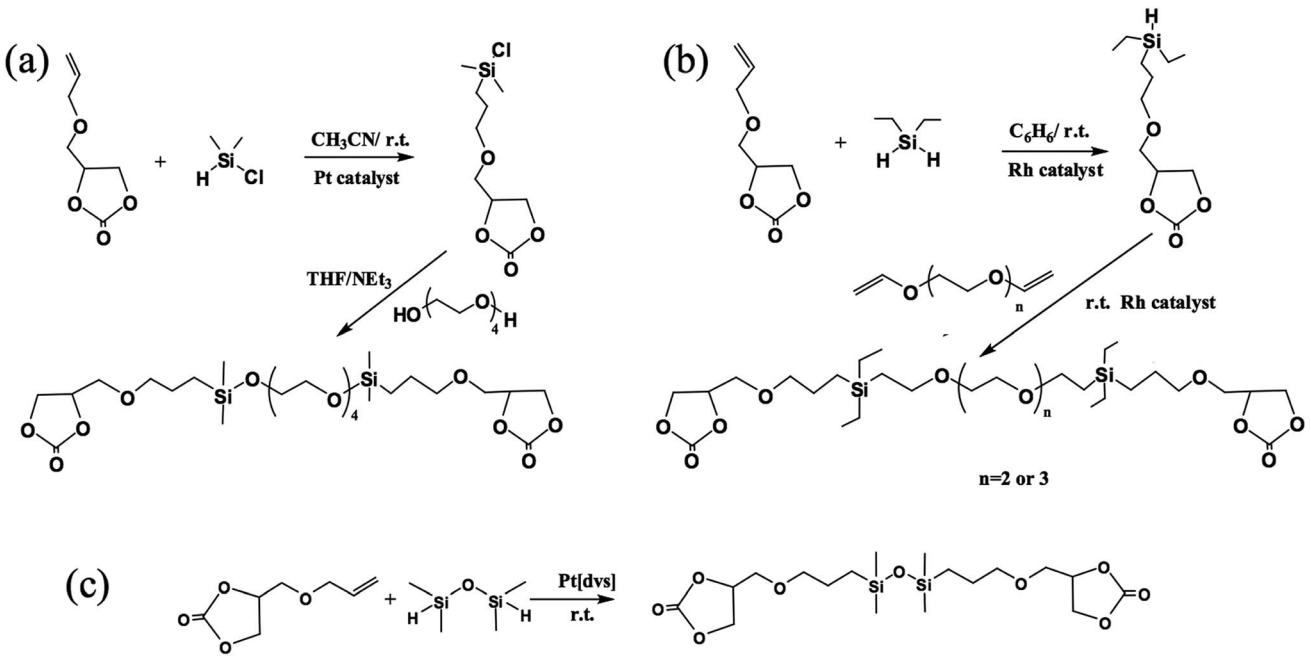

Scheme 2 Synthesis of oligomer plasticizers (a) OP62, (b) OP73 ($n = 2$) and OP67 ($n = 3$), and (c) OP89.

catalyst [$RhCl(PPh_3)_3$] suggested by Hartwig *et al.* exhibited better catalyzing capability.[29] The hydrosilylation for the second SiH groups on the same Si atom didn't start until all the first SiH groups were consumed, as confirmed by ^1H NMR. The synthesis of OP89 (Scheme 2(c)) is straightforward. The reaction was impossible to stop at the monosubstitution state, even with excess dihydrosilane.

The OP and CPP samples were blended with a tetraphenyl borate – Li polysiloxane single-ion conductor synthesized in our previous work, having 14 mol% tetraphenyl borate-86 mol% cyclic carbonate and Li^+ counterions.[13] The weight fraction of the ionomer in all mixtures is $w = 20$ wt%. To prepare the mixtures, the ionomer and plasticizer were dissolved in a common solvent, acetone, and the solvent was evaporated first *via* rotovap and then the blends were put in a vacuum oven at 80 °C. Since OP evaporates slowly in vacuum at 80 °C, 5–10 wt% extra OP was added in the common solvent, and the sample was weighed every 2–3 hours after introducing into the vacuum oven to record the weight loss of OP with time. More than 10 hours in the vacuum oven were required to evaporate the extra OP and obtain the target content of 20 wt% ionomer.

Glass transition temperature

Glass transition temperatures (T_g) of CPP and OP are plotted against f and f', respectively, in Fig. 1 in filled symbols. T_g of CPP increases with polar carbonate content f. The overall trend is well predicted by the Fox equation (thick solid curve in Fig. 1):

$$\frac{1}{T_g} = \frac{f}{T_{g,CPP100}} + \frac{1-f}{T_{g,CPP0}} \quad (1)$$

T_gs of OPs are lower than T_gs of CPPs and the Fox equation prediction. The Fox eqn (1) can predict T_gs of the random copolymers from the T_gs of the two homopolymers when the copolymers and homopolymers have (1) similar chain sizes and thus an effect of chain ends, known to cause extra free volume, has equal contribution of T_g, or (2) sufficiently large chain sizes and thus an effect of chain ends is negligible. Since OPs are oligomers for which chain ends play a big role in reducing T_g, the OPs having T_g well below the Fox equation of the much longer homopolymers (CPP0 and CPP100) is reasonable. This argument also explains the overall trend that T_g is further below the Fox prediction at higher f': considering that each OP molecule contains identically two carbonate end groups, larger f' simply means shorter chain and accordingly stronger chain

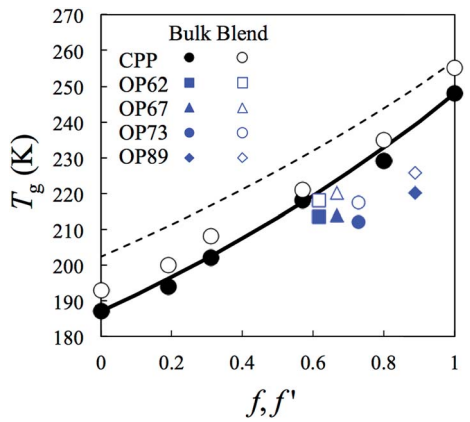

Fig. 1 Glass transition temperatures T_g of CPP and OP plasticizers against f and f', respectively (filled symbols). T_g of resulting blends (80 wt% plasticizer and 20 wt% ionomer) is added for comparison (open symbols). Thick solid and thin dashed curves show predictions of Fox eqn (1) and (2), respectively.

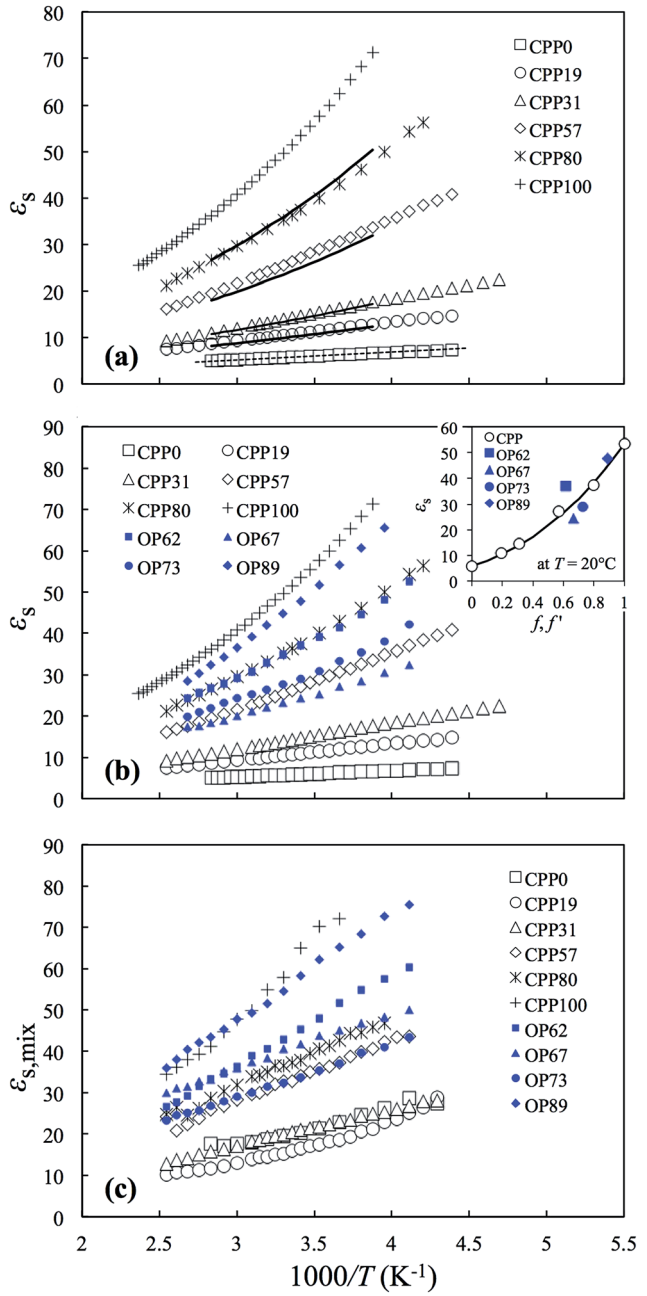

Fig. 2 (a) Temperature dependences of static dielectric constant ε_s of CPPs (in symbols) and the predictions by the Landau and Lifshitz mixing rule (eqn (3), solid curves) and the Onsager equation for CPP0 (dotted line). (b) Comparison of dielectric constants of the CPPs (in black symbols) and OPs (in blue symbols). Inset: static dielectric constant ε_s at $T = 20$ °C increases with the fraction of carbonate units f for the six CPPs (open symbols). The solid curve is the Landau and Lifshitz mixing rule, eqn (3). ε_s *vs.* f' of the four OPs are added for comparison (filled symbols). The significantly larger ε_s of OP62 seems to play a role in its superior conductivity. (c) Dielectric constant of mixtures of 20 wt% of 14 mol% lithium tetraphenyl borate/86 mol% cyclic carbonate random copolymer ionomer[13] with 80 wt% of the various plasticizers.

end effect. Blended with 20 wt% ionomer with significantly higher T_g (=301 K), the mixtures display only ~5 K higher T_g than the plasticizers alone. The increase is less than the Fox prediction of eqn (2) shown as the dashed curve in Fig. 1, suggesting that an ion-solvating effect lowers T_g, which is more obvious when EO units are present in the plasticizer.

$$\frac{1}{T_g} = \frac{w}{T_{g,\text{ionomer}}} + \frac{f(1-w)}{T_{g,\text{CPP100}}} + \frac{(1-f)(1-w)}{T_{g,\text{CPP0}}} \quad (2)$$

Dielectric constant

In Fig. 2(a), the static dielectric constant ε_s of CPP increases with content of polar cyclic carbonate groups. The ε_s values of the four CPP random copolymers can be predicted from those of the two CPP homopolymers (CPP100 and CPP0) very well with the Landau and Lifshitz mixing rule,[30] at all temperatures in the liquid state (solid curves in Fig. 2(a) and the inset of Fig. 2(b)).

$$\varepsilon_s^{1/3} = f\varepsilon_{s,\text{CPP100}}^{1/3} + (1-f)\varepsilon_{s,\text{CPP0}}^{1/3} \quad (3)$$

While the CPP0 homopolymer perfectly obeys the Onsager equation (dotted line in Fig. 2(a))[31] the CPP100 homopolymer exhibits strong curvature for reasons that are not apparent, yet still the Landau–Lifshitz mixing rule works perfectly for all four random copolymers.

Fig. 2(b) compares the static dielectric constants ε_s of the four OPs and six CPPs, which are comparable when f' and f are comparable (compare the four OPs ($f' = 62\%$ to 89%) to CPPs of $f = 57\%$ and 80% in Fig. 2(b)). This feature is more clearly seen in the inset, where ε_s of CPPs and OPs at $T = 20$ °C are plotted against f and f', respectively.

In the Fig. 2(b) inset, ε_s of the OPs scatters closely around the Landau and Lifshitz curve, meaning the dielectric constant for both CPPs and OPs is governed by the carbonate : EO ratio. The considerable scattering should be related to the detailed molecular structure. Considering ε_s here reflects a response of the dipole moments to applied electric field, it should be related to not only the density of dipoles but also how the dipoles interact with each other, *i.e.* dipole–dipole correlations. The latter effect should rely on the molecular structure, in particular an energy barrier for dipole rotation. For example, OP62 has ε_s considerably higher than that expected from f'. The reason could be related to the ultra-flexible Si–O bond that allows the polar carbonate groups of OP62 to respond more easily to an applied electric field.[32–35] This argument is in accordance with the observation that OP62 and OP89 having Si–O bonds exhibit ε_s higher than those of CPPs, while OP67 and OP73 having no Si–O bond exhibit ε_s lower than those of the CPPs. The dielectric constants of the mixtures with 20 wt% ionomer are shown in Fig. 2(c), with blend dielectric constant increasing with cyclic carbonate content.

Fig. 3(a) shows the temperature dependence of ionic conductivity σ_{DC} of the ionomer (red symbols) and its 20 wt% mixtures with CPP (black symbols) and OP (blue symbols). For CPP mixtures, the conductivity shows an interesting crossover,

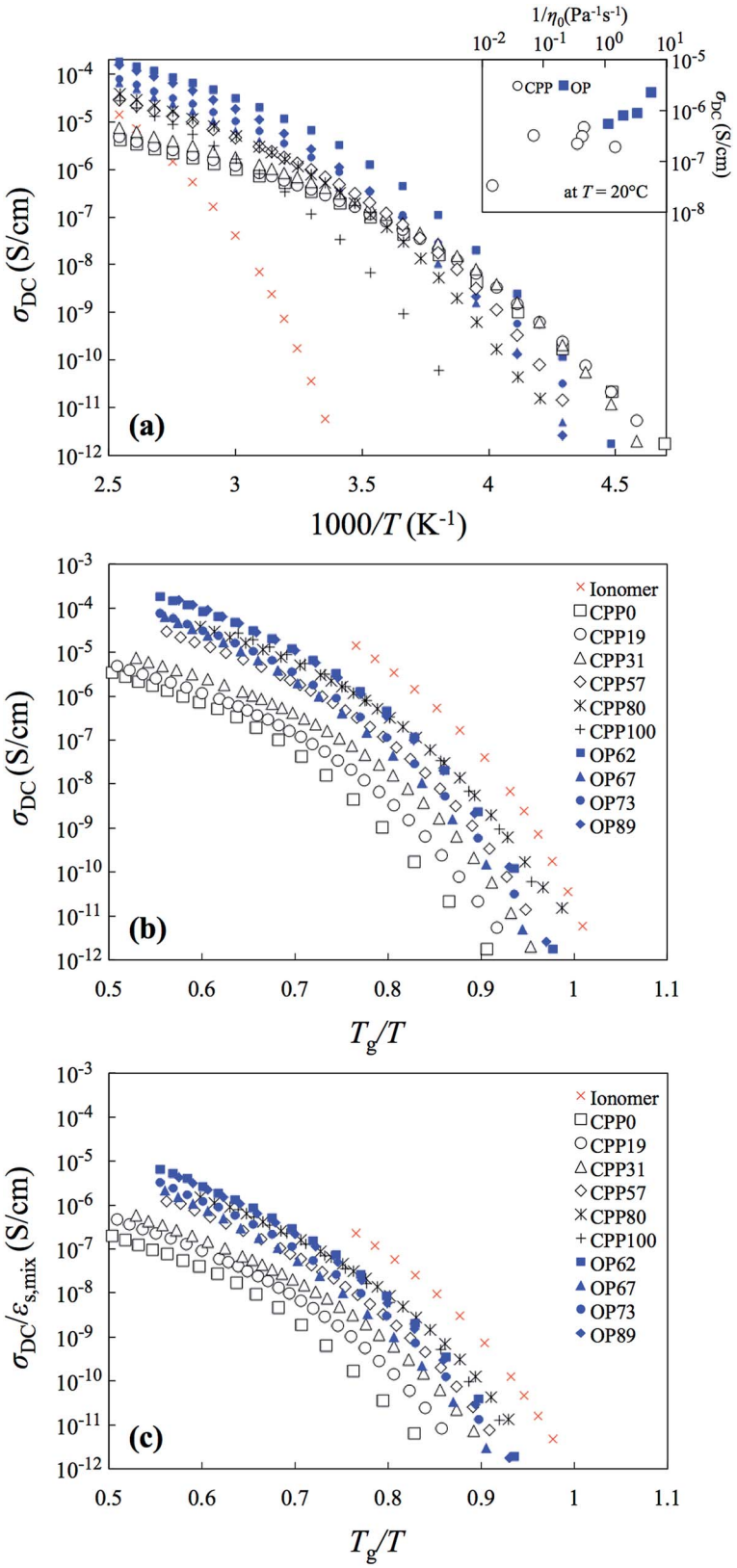

Fig. 3 (a) Temperature dependence of ionic conductivity for the ionomer (red × symbols) and its blends with CPP (black symbols) and OP (blue symbols) at 20 wt% ionomer. Inset: σ_{DC} *versus* $1/\eta_0$ at $T = 20$ °C. (b) T_g/T dependence of the ionic conductivity. (c) T_g/T dependence of ionic conductivity divided by static dielectric constant.

Table 1 Molecular weight M, glass transition temperature T_g, and 20 °C values of static dielectric constant ε_s and zero-shear viscosity η_0 of plasticizers

	CPP0	CPP19	CPP31	CPP57	CPP80	CPP100	OP62	OP67	OP73	OP89
M^a (g mol^{-1})	12 700	12 400	12 200	11 800	11 400	11 100	626	695	651	450
T_g (K)	187	194	202	218	229	248	213	214	212	220
ε_s	5.9	11	15	27	38	54	37	24	29	48
η_0 (Pa s)	0.70	2.83	2.39	2.21	14.8	68.6	0.18	0.87	0.51	0.30

[a] Number-average molecular weight of CPP, calculated from f, assuming number-average DP = 52.

increasing with f at sufficiently high T while decreasing with f at sufficiently low T. This result reflects a tradeoff between reducing T_g *via* increasing the EO content (Fig. 1) and increasing ε_s *via* increasing the cyclic carbonate content (Fig. 2). The reduction of T_g (faster segmental motion) boosts ionic mobility and dominates at low T close to T_g. The increase of ε_s softens ionic interactions and facilitates ion dissociation; this effect dominates at high T, sufficiently far above T_g. The effect of ε_s increasing with cyclic carbonate content is more clearly seen in Fig. 3(b) where temperature has been normalized by T_g. At constant T_g/T, σ_{DC} increases with f for the CPP mixtures. This trend is also seen in the OP mixtures: the conductivity decreases in the order OP89 ∼ OP62 > OP73 > OP67, in accordance with the order of their ε_s.

In Fig. 3(a), σ_{DC} is larger for the OP mixtures than the CPP samples even if f and f' are comparable, reflecting that the smaller OP molecules exhibit lower viscosity than the larger CPP molecules (Table 1). The lower viscosity is due partly to the lower T_g for OPs seen in Fig. 1, and also partly to the smaller size of the OPs. In accordance with this argument, the inset of Fig. 3(a) shows an overall trend that σ_{DC} increases with the inverse of zero-shear viscosity η_0 at $T = 20$ °C (see Table 1), well-known as Walden's rule.[36] Fig. 3(c) shows that dividing conductivity by the dielectric constant of the mixture does not quite reduce all data to a common curve plotted against T_g/T.

OP62 appears to be the best choice of plasticizer at any temperature above 250 K, of the ten samples studied here (see Fig. 3(a)). This plasticizer is the only one with Si–O–C linkages, which are polar, flexible and unfortunately easily hydrolyzed in the presence of moisture. OP62 has dielectric constant 30% larger than the Landau–Lifshitz prediction (see inset of Fig. 2(b)), and by far the lowest viscosity (Table 1) even though T_g is only 10 K lower than predicted by the Fox equation (Fig. 1).

Conclusions

Two groups of low-volatility plasticizers are synthesized: both are composed of highly polar cyclic carbonate and more flexible short ethylene oxide chains. Those novel low-volatility plasticizers might replace the organic carbonate solvent used in the lithium-ion battery industry to eliminate the safety problems existing in current rechargeable lithium-ion batteries. The combination of ethylene oxide and cyclic carbonate can tune T_g and dielectric constant to optimize σ_{DC}. The final performance of the plasticizers is decided by their chemical structure, consequently T_g, dielectric constant and viscosity. The best plasticizer OP62 has the lowest viscosity, the most flexible structure and nearly the highest dielectric constant. Polymer single-ion conductor blends containing those plasticizers and a borate ionomer have conductivity up to 2×10^{-5} S cm^{-1} at 25 °C. By mixing with low-volatility polar plasticizers, these ionomers are potential candidates to make safer gel polymer electrolytes for lithium-ion rechargeable battery separators.

Acknowledgements

The authors gratefully acknowledge the financial support of the Department of Energy under Grant BES-DE-FG02-07ER46409. Janna Maranas, Karl Mueller (both at Penn State) and Karen Winey from the University of Pennsylvania are thanked for helpful discussions.

References

1 K. E. Thomas, S. E. Sloop, J. B. Kerr and J. Newman, *J. Power Sources*, 2000, **89**, 132–138.
2 P. V. Wright, *MRS Bull.*, 2002, **27**, 597–602.
3 D. Fragiadakis, S. Dou, R. H. Colby and J. Runt, *J. Chem. Phys.*, 2009, **130**, 064907.
4 W. Wang, G. J. Tudryn, R. H. Colby and K. I. Winey, *J. Am. Chem. Soc.*, 2011, **133**, 10826–10831.
5 G. J. Tudryn, M. V. O'Reilly, S. C. Dou, D. R. King, K. I. Winey, J. Runt and R. H. Colby, *Macromolecules*, 2012, **45**, 3962–3973.
6 Q. Chen, H. Masser, H.-S. Shiau, S. Liang, J. Runt, P. C. Painter and R. H. Colby, *Macromolecules*, 2014, **47**, 3635–3644.
7 N. Matsumi, K. Sugai, K. Sakamoto, T. Mizumo and H. Ohno, *Macromolecules*, 2005, **38**, 4951–4954.
8 X. G. Sun and J. B. Kerr, *Macromolecules*, 2006, **39**, 362–372.
9 B. S. Qin, Z. H. Liu, G. L. Ding, Y. L. Duan, C. J. Zhang and G. L. Cui, *Electrochim. Acta*, 2014, **141**, 167–172.
10 Y. S. Zhu, S. Y. Xiao, Y. Shi, Y. Q. Yang and Y. P. Wu, *J. Mater. Chem. A*, 2013, **1**, 7790–7797.
11 T. Fujinami, M. A. Mehta, K. Sugie and K. Mori, *Electrochim. Acta*, 2000, **45**, 1181–1186.
12 W. Liu, M. J. Janik and R. H. Colby, in *Polymers for Energy Storage and Delivery: Polyelectrolytes for Batteries and Fuel Cells*, ed. K. A. Page, C. L. Soles and J. Runt, ACS Symp. Series, 2012, vol. 1096, ch. 2, pp. 19–44.
13 S. Liang, U. H. Choi, W. Liu, J. Runt and R. H. Colby, *Chem. Mater.*, 2012, **24**, 2316–2323.

14 J. Y. Song, Y. Y. Wang and C. C. Wan, *J. Power Sources*, 1999, **77**, 183–197.
15 A. M. Stephan, *Eur. Polym. J.*, 2006, **42**, 21–42.
16 P. Zhang, L. L. Li, D. N. He, Y. P. Wu and M. Shimizu, *Acta Polym. Sin.*, 2011, 125–131.
17 M. Forsyth, J. Sun, F. Zhou and D. R. MacFarlane, *Electrochim. Acta*, 2003, **48**, 2129–2136.
18 K.-D. Kreuer, A. Wohlfarth, C. C. de Araujo, A. Fuchs and J. Maier, *ChemPhysChem*, 2011, **12**, 2558–2560.
19 Y. V. Baskakova, O. V. Yarmolenko and O. N. Efimov, *Russ. Chem. Rev.*, 2012, **81**, 367–380.
20 J. R. MacCallum and C. A. Vincent, *Polymer Electrolyte Reviews*, Springer, 1987.
21 H.-S. Shiau, W. Liu, R. H. Colby and M. J. Janik, *J. Chem. Phys.*, 2013, **139**, 204905.
22 U. H. Choi, S. Liang, M. V. O'Reilly, K. I. Winey, J. Runt and R. H. Colby, *Macromolecules*, 2014, **47**, 3145–3153.
23 D. K. Pradhan, R. N. P. Choudhary and B. K. Samantaray, *Mater. Chem. Phys.*, 2009, **115**, 557–561.
24 Y. Ito, K. Kanehori, K. Miyauchi and T. Kudo, *J. Mater. Sci.*, 1987, **22**, 1845–1849.
25 J. Y. Lee, Y. M. Lee, B. Bhattacharya, Y. C. Nho and J. K. Park, *J. Solid State Electrochem.*, 2010, **14**, 1445–1449.
26 F. Kaneko, S. Wada, M. Nakayama, M. Wakihara, J. Koki and S. Kuroki, *Adv. Funct. Mater.*, 2009, **19**, 918–925.
27 Y. W. Li, J. W. Wang, J. W. Tang, Y. P. Liu and Y. D. He, *J. Power Sources*, 2009, **187**, 305–311.
28 M. V. O'Reilly, H. Masser, D. R. King, P. C. Painter, R. H. Colby, K. I. Winey and J. Runt, *Polymer*, 2015, **59**, 133–143.
29 N. Tsukada and J. F. Hartwig, *J. Am. Chem. Soc.*, 2005, **127**, 5022–5023.
30 L. D. Landau and E. M. Lifshitz, *Electrodynamics of Continuous Media*, Pergamon Press, Oxford, 1963.
31 L. Onsager, *J. Am. Chem. Soc.*, 1936, **58**, 1486–1493.
32 Z. Zhang, D. Sherlock, R. West, R. West, K. Amine and L. J. Lyons, *Macromolecules*, 2003, **36**, 9176–9180.
33 Z. Zhang, L. J. Lyons, R. West, K. Amine and R. West, *Silicon Chem.*, 2005, **3**, 259–266.
34 N. A. A. Rossi and R. West, *Polym. Int.*, 2009, **58**, 267–272.
35 B. Oh, R. C. West and K. Amine, *US Pat.*, 7,588,859. 2009.
36 P. Z. Walden, *Phys. Chem.*, 1906, **55**, 207–246.

